Elucidating the Role of a Tetrafluoroborate-based Ionic Liquid at the n-Type Oxide/Perovskite Interface

Nakita K. Noel,[1,2*] Severin N. Habisreutinger,[3] Bernard Wenger,[4] Yen-Hung Lin,[4] Fengyu Zhang,[2] Jay B. Patel,[4] Antoine Kahn,[2] Michael B. Johnston,[4] Henry J. Snaith.[4*]

Dr. N. K. Noel
Princeton Institute for the Science and Technology of Materials, Princeton University
Princeton, NJ, 08544, USA
E-mail: nnoel@princeton.edu

Dr. N. K. Noel, F. Zhang, Prof. A. Kahn
Department of Electrical Engineering, Princeton University
Princeton, NJ, 08544, USA

Dr. S. N. Habisreutinger
National Renewable Energy Laboratory
Golden, Colorado, 80401, USA

Dr. B. Wenger, Dr. Y. H. Lin, Dr. J. B. Patel, Prof. M. B. Johnston, Prof. H. J. Snaith
Clarendon Laboratory, Department of Physics, University of Oxford
Parks Road, Oxford, OX1 3PU, UK
Email: henry.snaith@physics.ox.ac.uk

Keywords: perovskite solar cell, reduced defect density, ionic liquids, Fermi level, time-resolved microwave conductivity

Abstract:

Halide perovskites are currently one of the most heavily researched emerging photovoltaic materials. Despite achieving remarkable power conversion efficiencies, perovskite solar cells have not yet achieved their full potential, with the interfaces between the perovskite and the charge-selective layers being where most recombination losses occur. In this study we employ a fluorinated ionic liquid (IL) to modify the perovskite/SnO_2 interface. Using Kelvin probe and

Pursuant to the DOE Public Access Plan, this document represents the authors' peer-reviewed, accepted manuscript.
The published version of the article is available from the relevant publisher.

photoelectron spectroscopy measurements, we show that depositing the perovskite onto an IL-treated substrate results in the crystallisation of a perovskite film which has a more n-type character, evidenced by a decrease of the work function and a shift of the Fermi level towards the conduction band. We use photoluminescence spectroscopy and time-resolved microwave conductivity to investigate the optoelectronic properties of the perovskite grown on neat and IL-modified surfaces and find that the modified substrate yields a perovskite film which exhibits an order of magnitude lower trap density than the control. When incorporated into solar cells, this interface modification results in a reduction in the current-voltage hysteresis and an improvement in device performance, with the best performing devices achieving steady-state PCEs exceeding 20%.

1. Introduction

From their inception in 2009, photovoltaic devices based on halide perovskites have undergone rapid increases in power conversion efficiency (PCE), from just over 3%[1] to certified values exceeding 25%.[2] Initially viewed solely as a promising absorber material due to their high absorption coefficients, researchers have since shown that halide perovskites also possess properties such as low exciton binding energies, and long-range, ambipolar charge transport.[3–7] These excellent material characteristics have led to an evolution in the architecture of perovskite solar cells from the use of an electron-conducting mesoporous scaffold to help support charge separation,[8] to an insulating scaffold,[3,9] to a thin-solid film of perovskite material sandwiched between electron and hole selective layers.[10,11]

The divergence from the mesoporous scaffold made it significantly harder to form continuous, uniform perovskite layers on a desired substrate.[10] This generated intense research interest into the control and manipulation of the crystallisation kinetics of perovskite materials, resulting in the development of numerous methods and interventions by which smooth, high-quality perovskite films can be deposited.[10–16] The improvements in the processing of perovskite thin-films were integral to the tremendous progress which has, thus far, been made in perovskite optoelectronic devices.

Unlike most other high-quality semiconductor materials, halide perovskites are remarkably defect-tolerant, with most harmful defects in thin-films being located at the grain boundaries and surfaces, with significant interfacial recombination also occurring at the heterojunctions

Pursuant to the DOE Public Access Plan, this document represents the authors' peer-reviewed, accepted manuscript.
The published version of the article is available from the relevant publisher.

between the perovskite absorber layers and other materials in the device stacks.[17–19] In perovskite photovoltaics for example, these defects and recombination pathways limit the open-circuit voltage of the devices by increasing non-radiative recombination of charge-carriers.[20] Consequently, passivation of these defects as well as the judicious tailoring of the interfaces between the perovskite and charge selective layers, are important strategies for reducing non-radiative recombination losses, and thus improving device performance.[20–25] Improving interfaces in perovskite cells can be achieved by chemical passivation of the perovskite surface,[16,21,22,26,27] or through tailoring the charge-selective layers to facilitate better forward carrier transfer.[15,23,25,28–30] The latter can be readily overcome by adopting various approaches that have been reported in the literature, such as the introduction of a work function modifier for example,[31] and deliberate and thoughtful selection of the charge-transport layers, with the expressed goal of minimising interfacial recombination. Additionally, these methods often lead to improved device stability.[15,32]

A typical chemical passivation approach to reducing defects in perovskite thin-films involves a post-treatment of the film with a material which binds to under-coordinated sites on the perovskite surfaces, effectively removing some of the sites at which photogenerated charge carriers are trapped and are subsequently lost to non-radiative recombination.[21,22] More recently, we have demonstrated p-type doping of the perovskite surface, which is an additional route to suppressing recombination at the perovskite/HTM interface.[24] In cases where a "passivating" agent is added directly to the precursor solution, the resulting improvement in the optoelectronic properties of the film is often due to the additive mediating crystallisation such that the resulting film has fewer grain boundaries and surface defects, for example through altering the size and concentration of colloids in the solution.[15,33] Examples of this are: solvent mixtures, and the addition of amines, acids, or excess ammonium halides to the precursor solution.[15,33–36] Improvements in the device performance have also been achieved by changing the electron selective layers in the device stack. For example, modifying the surface of TiO_2 by inserting thin layers of organic material (such as C_{60} or PCBM), or in other cases, entirely replacing TiO_2 with SnO_2 has been shown to improve charge extraction and reduce interfacial recombination.[28,37,38]

Ionic liquids (ILs) have been reported to improve the performance of perovskite solar cells, and have been used both as an additive to the perovskite precursor solution, where it is employed to tune crystallisation kinetics of the perovskite film,[39,40] and as an interlayer between TiO_2

Pursuant to the DOE Public Access Plan, this document represents the authors' peer-reviewed, accepted manuscript.
The published version of the article is available from the relevant publisher.

and the perovskite material.[41] Chang et al. reported the elimination of hysteresis in the current-voltage (*JV*) curves when TiO_2 is treated with 1-butyl-3-methylimidazolium tetrafluoroborate ($BMIMBF_4$).[41] In that work, it was shown that treating the TiO_2 surface with $BMIMBF_4$ results in more efficient electron extraction, which is attributed to a decrease in the work function of the TiO_2 which improves its energy level alignment with the perovskite, as well as an increase in electron mobility of the titania due to the passivation of trap states on the TiO_2 surface. The authors postulate that these changes to the TiO_2 layer result in the elimination of hysteresis in the *JV* curves due to enhanced charge extraction and the suppression of charge accumulation at the interface. Similar work had also previously been carried out by Wu et al. using another fluorinated IL, 1-ethyl-3-methylimidazolium hexafluorophosphate ($EMIMPF_6$).[42] There, the authors also show that although the best performance is achieved when a double layer of TiO_2/IL is used, a respectable performance can be achieved simply by treating the surface of the electrode (in this case FTO) with the IL. Similar results have also been reported for flexible perovskite solar cells, where an IL was used in lieu of a typical electron selective layer.[43] Aside from being used to modify inorganic charge transport layers, deposition of ILs on the surface of a PCBM electron transporting layer (in lieu of the more commonly used bathocuproine interlayer) has also been shown to improve the performance and stability of inverted (p-i-n) perovskite solar cells.[44] Additionally, recent work using ILs in perovskite solar cells has yielded considerable improvements to the long-term stability of these devices through the incorporation of $BMIMBF_4$ into the perovskite precursor solution in one case,[45] and 4-imidazoleacetic acid hydrochloride as an interface modifier in the other.[46]

In the vast majority of these studies where the IL is not thought to strongly affect the crystallization kinetics of the perovskite, the focus has been placed mainly on the interaction between the IL and the metal oxide, largely neglecting any direct interaction between the IL and the perovskite layer. In this study, we investigate the interaction between the ionic liquid $BMIMBF_4$ and both the electron transport layer (ETL), in this case SnO_2, and the mixed-cation lead mixed-halide perovskite, $FA_{0.83}MA_{0.17}Pb(I_{0.83}Br_{0.17})_3$. We confirm that, as previously reported, treating metal oxides with $BMIMBF_4$ results in their surface becoming more n-type (the work function decreases), but importantly we also show that there is a marked effect on the perovskite layer deposited on top of the IL, namely that the perovskite Fermi level shifts towards the conduction band. Additionally, we show that the IL itself interacts with the perovskite layer, reducing the trap densities in the material. We propose that it is the confluence of these two effects, rather than solely improvements to the metal oxide layer and its energetic

Pursuant to the DOE Public Access Plan, this document represents the authors' peer-reviewed, accepted manuscript.
The published version of the article is available from the relevant publisher.

alignment with the perovskite absorber layer, that results in the improved performance of perovskite solar cells with IL-modified charge electron transport layers.

2. Results and Discussion

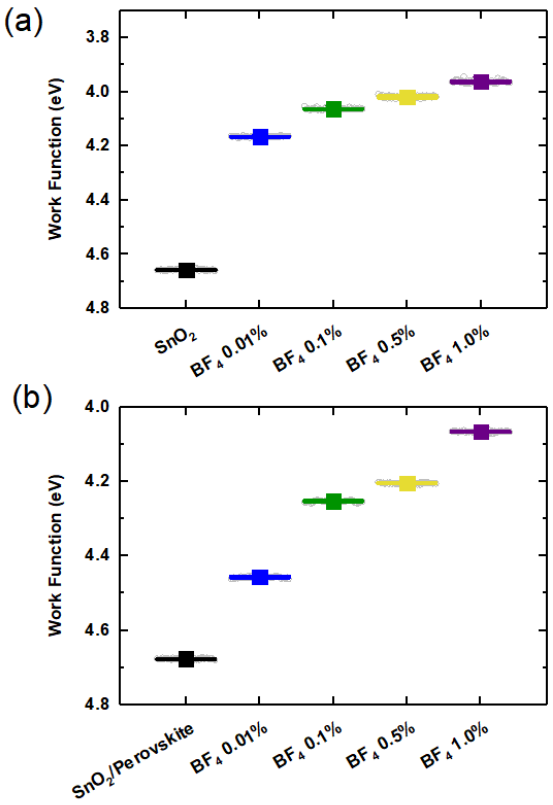

Figure 1. Kelvin Probe Measurements. Work function of (a) SnO_2 films treated with various concentrations of $BMIMBF_4$ and (b) $FA_{0.83}MA_{0.17}(PbI_{0.83}Br_{0.17})_3$ films deposited onto SnO_2 films which have been treated with various concentrations of $BMIMBF_4$.

In most reports of IL-modified metal oxides in n-i-p cells, TiO_2 has been the electron-transport layer (ETL) of choice.[14,41,42] However, several studies have shown that due to improved energy alignment and reduced interfacial recombination, SnO_2 is a superior choice of ETL in planar heterojunction perovskite solar cells, resulting in reduced hysteresis and better device performance.[37,38] Consequently, in this study we utilise SnO_2 as the ETL and investigate whether similar results are obtained using this material. Firstly, *via* contact potential difference (CPD) measurements using a Kelvin Probe (KP) (**Figure 1a**), we investigate changes in the work function (WF) of the SnO_2 when the surface is treated with various concentrations of $BMIMBF_4$ diluted in methanol. We note here that the control sample has been treated with

Pursuant to the DOE Public Access Plan, this document represents the authors' peer-reviewed, accepted manuscript.
The published version of the article is available from the relevant publisher.

methanol in the same fashion, to rule out any possible changes due to any interaction between the solvent and the SnO_2 layer. As has been previously reported with TiO_2,[41] we observe that treating the surface of SnO_2 results in a reduction in the WF of the film. Interestingly, this also causes a significant and corresponding change in the WF (**Figure 1b**) of the perovskite film that is subsequently deposited on top of the treated SnO_2, indicating that the presence of $BMIMBF_4$ at the metal oxide/perovskite interface may also influence the electronic properties of the perovskite material.

In the case of the SnO_2 layer, the decrease in WF change is likely due to a surface dipole caused by the deposition of the IL, with the BF_4^- interacting with the surface, and the $BMIM^+$ pointing away from the surface. However, we would not expect the effect of a dipole to propagate through 500 nm of crystalline perovskite material. The WF change at the perovskite surface follows to some degree that of the substrate and is further investigated below with photoelectron spectroscopy. It is reminiscent of changes observed, for example, on $MAPbI_3$ on TiO_2 vs. NiO,[47,48] or other materials with similarly low intrinsic carrier concentrations, such as organic semiconductors, deposited on substrates with very different WFs.[49] To ascertain whether the observed change in the work function is linked to any macroscopic structural changes in the perovskite film, we remove the SnO_2 ETL and investigate whether crystallising the perovskite on the IL layer results in structural/morphological changes in the material. To do this, we carry out X-ray diffraction (XRD), scanning electron microscopy (SEM) and optical absorption measurements on films deposited on bare and IL-treated FTO, and show the results of these investigations in **Figures S1** and **S2**. In the XRD and SEM measurements, we find negligible differences between films grown on bare and treated surfaces, and therefore exclude structural or morphological changes as being responsible for the change in the perovskite WF which we observe. In the absorption measurements, we also observe very little difference.

Pursuant to the DOE Public Access Plan, this document represents the authors' peer-reviewed, accepted manuscript.
The published version of the article is available from the relevant publisher.

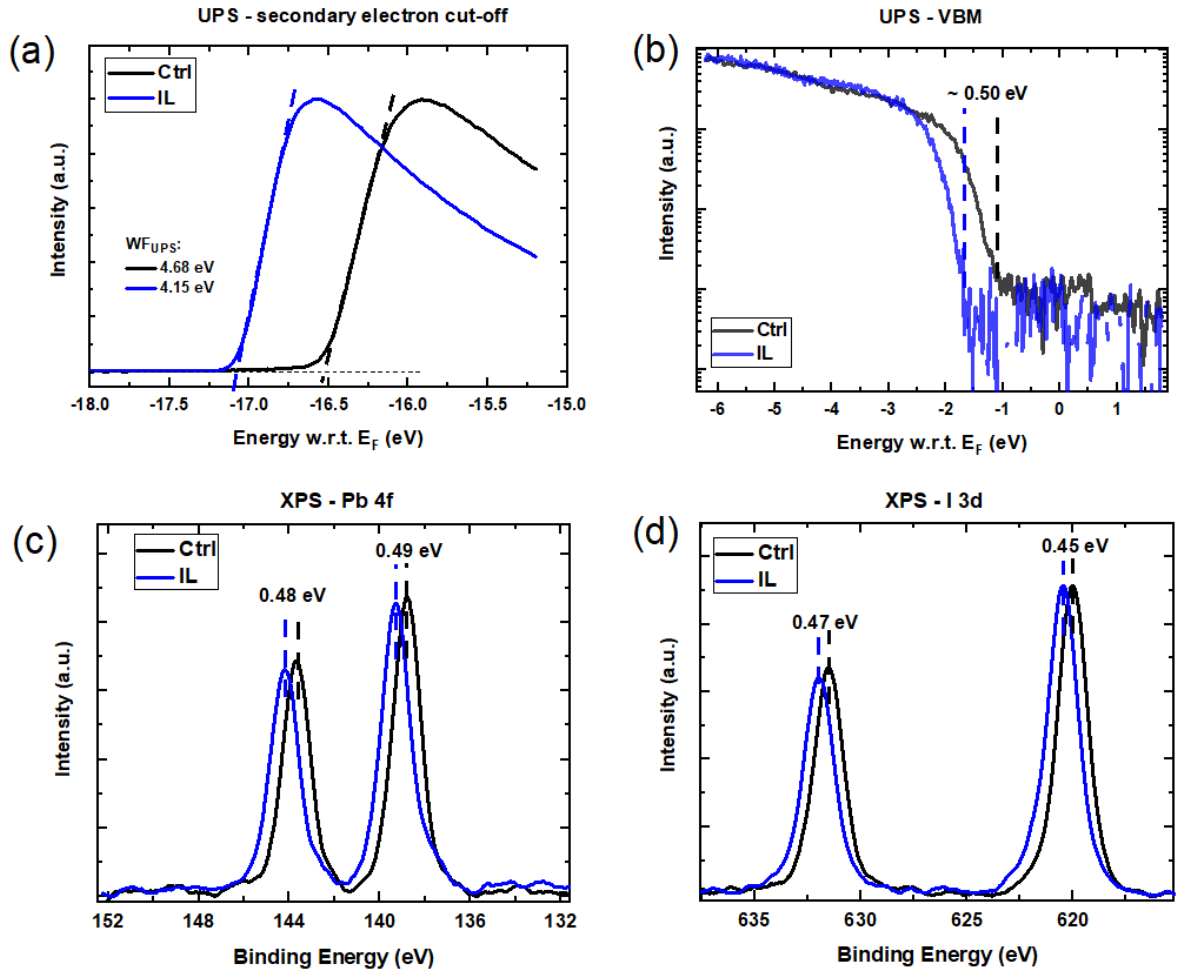

Figure 2. Photoelectron Spectroscopy Measurements. (a) Secondary electron cut-off and (b) valence band maxima of $FA_{0.83}MA_{0.17}Pb(I_{0.83}Br_{0.17})_3$ perovskite thin-films grown on bare (Ctrl) and IL-treated ITO (IL). XPS spectra of the (a) Pb 4f and (d) I 3d regions of films investigated in (a) and (b).

To further probe the effects of the IL on the electronic properties of the perovskite, we carry out ultraviolet and X-ray photoelectron spectroscopy (UPS and XPS, respectively), and show this data in **Figure 2**. The UPS measurements were conducted using a standard He I radiation line, with the photoemission signal being measured with both a linear and a logarithmic detection ratemeter. As previously reported, the latter measurement allows for a more accurate determination of the position of the valence band maximum in 3D perovskite systems.[50] To rule out any changes in the perovskite sample due to irradiation, we measure the WF of the sample surface using KP before and after UPS and XPS measurements, and here, find the WF unchanged. From the UPS measurements, we find shifts of the secondary electron cut-off (Fig. 2a) and of the valence band states away from the Fermi level, E_F, or equivalently, a shift of the E_F towards the upper part of the gap (~ 0.5 eV) when the perovskite is crystallised on the IL-

Pursuant to the DOE Public Access Plan, this document represents the authors' peer-reviewed, accepted manuscript.
The published version of the article is available from the relevant publisher.

treated substrate, indicative of the formation of a more n-type material. This is also reflected in the Pb 4f and I 3d core level shifts (of approximately the same value) towards higher binding energy with respect to E_F, which we measure *via* XPS. We show the XPS survey spectra in **Figure S3**. These results suggest an interaction between the perovskite film and the $BMIMBF_4$-treated substrate on which it is crystallised, resulting in a change in the doping level of the perovskite, such that it becomes more n-type.

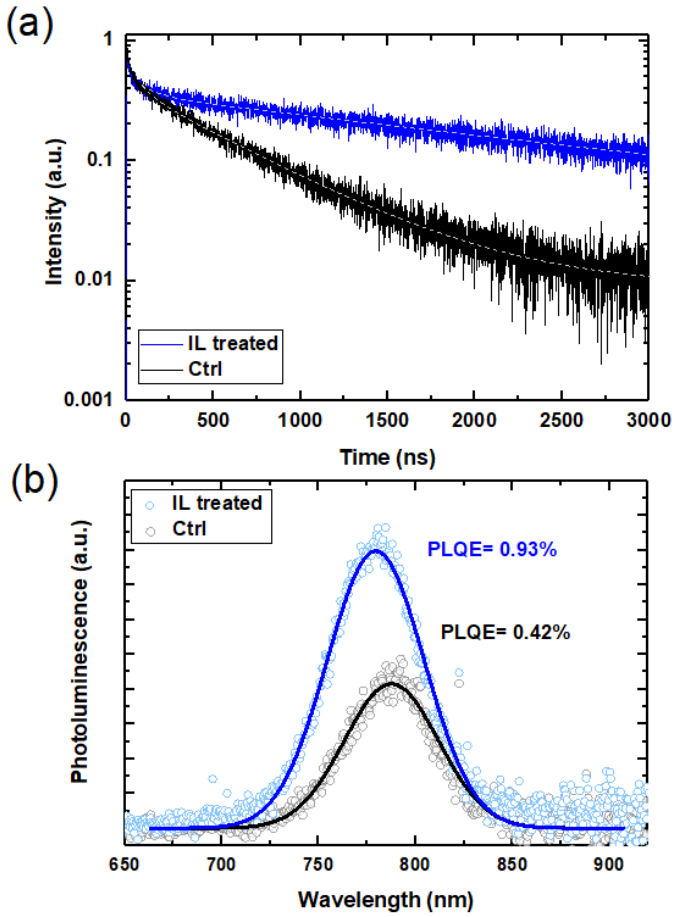

Figure 3. Photoluminescence Measurements. (a) Time-resolved photoluminescence of perovskite films grown on bare (ctrl) and $BMIMBF_4$-treated glass (IL-treated). Exponential fits are depicted with white dashed lines. Samples were excited with a 505 nm laser head (LDH-P-C-505), PicoQuant GmbH) pulsed at a frequency of 0.1 MHz with a fluence of ~30 nJ/cm^2. (b) Photoluminescence quantum efficiencies of perovskite films grown on bare and $BMIMBF_4$-treated glass.

Pursuant to the DOE Public Access Plan, this document represents the authors' peer-reviewed, accepted manuscript.
The published version of the article is available from the relevant publisher.

Changes in the doping levels are very likely to result in observable changes in the optoelectronic properties of the material. As such, we subsequently probe the optoelectronic quality of the films through photoluminescence (PL) measurements and show these results in **Figure 3**. Fig. 3a shows the time-resolved PL decays of perovskite films grown directly on bare glass, and on $BMIMBF_4$-treated glass. Here, we see that the sample where the perovskite is crystallised on top of the IL shows a significant increase in the PL lifetime compared to the perovskite crystallised on bare glass. This indicates a reduction in non-radiative recombination when the perovskite is crystallised on the IL. This is also confirmed through PL quantum efficiency measurements, in Fig. 3b, which show an increase in emission from these films. This data appears to be consistent with a reduction in the defect density of films which have been grown on the IL-treated substrate.

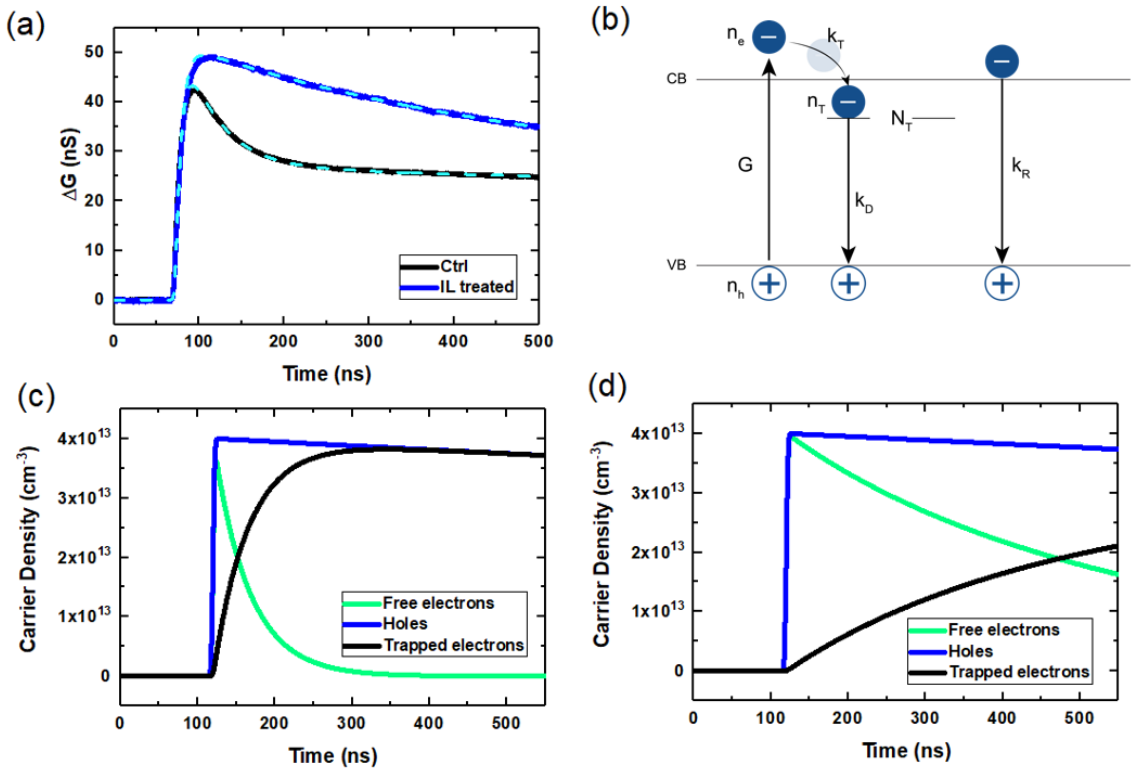

Figure 4. Time-resolved Microwave Conductivity. (a) Photoconductivity transients of representative perovskite films grown on bare quartz (ctrl) and $BMIMBF_4$-treated quartz (IL-treated). Overlaid are the corresponding simulated decays calculated with a simple kinetic model (dashed cyan traces). (b) Kinetic scheme of the different decay pathways for charge carriers after generation. Simulated decay dynamics of the three relevant carrier species (electrons, holes and trapped electrons) of the (c) control and (d) IL-treated samples.

Pursuant to the DOE Public Access Plan, this document represents the authors' peer-reviewed, accepted manuscript.
The published version of the article is available from the relevant publisher.

To further probe this difference, we carry out time-resolved microwave conductivity (TRMC) measurements on neat and IL-treated samples. We show this data in **Figure 4**. TRMC is a technique which can be used to probe both the mobility and availability of charges over time. This is done through first exciting a sample with a laser pulse and monitoring transient changes in the microwave (MW) field. Since the MW field interacts resonantly with mobile charge carriers, the attenuation of the field is proportional to the product of the number of charge carriers and their mobilities (full details and validation of the model are given in the experimental section). From this, we can extract a yield sum mobility product ($\phi\Sigma\mu$ where μ- mobility and ϕ- the ratio of free electron-hole pairs generated per photon absorbed]) and track this over time. The low exciton binding energy in halide perovskites, allows us to assume that under low excitation fluences, each photon generates a free electron and a corresponding free hole ($\phi = 1$) at low carrier concentration ($< 10^{17}$ cm^{-3}).[51] In good agreement with the photoluminescence data shown in Fig.3, we find that for the perovskite film grown on $BMIMBF_4$-treated quartz, the lifetime of the charge-carriers is considerably longer (Fig.4a).

	Control	IL treated
k_T (cm^{-3} s^{-1})	**3.0×10^{-9}**	**3.0×10^{-9}**
k_D (cm^{-3} s^{-1})	**2.0×10^{-9}**	**4.5×10^{-9}**
k_R (cm^{-3} s^{-1})	**6.0×10^{-10}**	**6.0×10^{-10}**
N_T (cm^{-3})	**7.9×10^{15}**	**7.9×10^{14}**

Table 1. Fit parameters extracted from the kinetic model used in Figure 4, where k_T- trapping rate constant, k_D- recombination rate constant, k_R- band-to-band recombination rate constant and N_T-trap density.

We can describe the charge carrier dynamics with a simple kinetic model (full details are given in the SI) where we can differentiate between photogenerated electrons and holes, and trapped electrons. The low fluence regime of the measurement allows us to limit the decay pathways to radiative and non-radiative recombination of those populations (Figure 4b). A laser pulse *G* photoexcites a density of *N* electrons into the conduction band yielding an equal number of holes populating the valence band. We assume that the dark carrier population (p_0) is much smaller than the photogenerated charge carrier concentration ($n_{e/p} >> p_0$). Based on the observation that the more n-type perovskite has a longer PL lifetime, we assume that the

Pursuant to the DOE Public Access Plan, this document represents the authors' peer-reviewed, accepted manuscript.
The published version of the article is available from the relevant publisher.

dominant trap species are electron traps. Many other studies have also indicated this to be the case.[52–54] Photogenerated electrons n_e have therefore two decay paths: 1) direct radiative recombination with holes in the valence band with the recombination rate k_R, and falling into traps N_T near the band edge at the trapping rate k_T. and 2) photogenerated holes n_p correspondingly decay due to direct band-to-band recombination k_R, and through non-radiative recombination, where trapped electrons depopulate the trap states with the rate constant k_D and recombine with holes at the valence band edge without emitting a photon. A third population of charges is the trapped electrons n_t which are generated through electron capture k_T and decay through electron escape, k_D. Through fitting the TRMC decays (Fig. 4a) to this kinetic model, we can extract the different decay rates and the trap density of the respective films. We show the parameters we determine from our fitting in Table 1 (fitting details and validation are given in the SI). Most notably, we find that the perovskite grown on the IL modified surface has an order of magnitude lower trap density than the control sample. This is consistent with the IL reducing the defect density in the perovskite film.

The experimental TRMC decays and their corresponding fits extracted from the kinetic model are shown in Figure 4a. The global fits across a range of fluences (**Fig. S7.2**) show excellent agreement with the experimental data. The quantitative data obtained from our model is shown in Table 1. Most notably, we find that the decay dynamics of the perovskite grown on the IL are consistent with an order of magnitude reduction of the trap density as compared to the control sample. Using this model, we can also obtain information on the decay dynamics of the three relevant charge carrier species considered (electrons, holes and trapped electrons). Here we see that for the IL-modified sample, the decay of free electrons is significantly slower (Figure 4c and d), and there is a decreased density of trapped electrons, due to a reduced availability of electron traps in the material. These results are consistent with the observation by Ramirez et al., who have demonstrated that the doping character of the perovskite has a strong influence on its optoelectronic properties.[55] Analogous to our observation, the authors suggest that a more n-type perovskite material exhibits improved optoelectronic properties because at equilibrium, more electron traps are more likely to be filled.[55]

At this point it is worth summarising the effects of the IL on the substrate and on the perovskite. Due to the fact that the deposition of the IL on the surface of a substrate introduces a dipole, it is likely that the IL will shift (in the same direction) the work function of almost any surface on which is it deposited. This has previously been observed for various types of materials such as

Pursuant to the DOE Public Access Plan, this document represents the authors' peer-reviewed, accepted manuscript.
The published version of the article is available from the relevant publisher.

polymers, where the deposition of the polymer on a variety of different substrates causes a shift in the work function of the substrate.[56] The dependence of the perovskite WF and E_F on the substrate it has been crystallised on has been well-documented in literature.[47,48,57] This is effectively what we see here in the WF shift of the perovskite, where as the WF of the substrate decreases, there is a corresponding decrease in the WF of the perovskite crystallised atop the substrate. This effect is often observed when investigating weakly (chemically) interactive interfaces between a substrate and a semiconductor with low intrinsic density of carriers, such as organics,[49] and indeed in perovskite materials,[47,48,58] where the work function of thin films (up to few hundreds of nm) of the semiconductor follows, to some extent, that of the substrate on which it has been deposited. The dominant idea behind this "substrate-dependent doping" phenomenon is that there is relative low charge-carrier density in the perovskite material, allowing for charge transfer from the substrate, which results in the equilibration of the Fermi level of the two materials. Consequently, the work function of the perovskite film, measured at its surface, will shift according to the work function of the substrate.

In attempt to isolate the effect of the IL on the perovskite material itself, we have carried out a series of PL and TRMC experiments on the perovskite deposited on quartz, and quartz which has been IL-treated in the same fashion as the conductive oxide. Here, we observe an increase in the PL lifetime and the PLQE of the films which have been deposited on the IL-treated substrate. Time-resolved PL (in the fluence regime investigated) gives information about the frequency of trap-assisted recombination events,[59] while the PLQE quantifies how much of that recombination is radiative. The experimental data which we have acquired suggests a reduction in the trap density of the material. This would decrease the trapping rates (increasing the PL lifetime), thus increasing the likelihood that a photogenerated electron and hole will recombine radiatively (increase in PLQE). This is indeed corroborated by the TRMC decays, where using a kinetic model, we show that crystallising the perovskite on top of the IL results in an order of magnitude reduced trap density. This is akin to a type of passivation effect however, in this case, it is more likely that crystallising the perovskite on top of the IL prevents the formation of trap states (likely at the perovskite/substrate interface) rather than a more classical view of defect passivation in perovskites, where post-crystallisation passivation is more often employed. This in itself has further implications for the observed Fermi-level shift, where it becomes difficult to disentangle the effect of the IL on the substrate, from the effect of the IL on the perovskite. The IL prevents the formation of (likely interfacial) defect states in the perovskite material, resulting in a more benign interface. Trap states which would otherwise

Pursuant to the DOE Public Access Plan, this document represents the authors' peer-reviewed, accepted manuscript.
The published version of the article is available from the relevant publisher.

occur at this interface can likely pin the Fermi level in the perovskite. The removal of these interface defects could thus allow the Fermi level of the perovskite to move toward the upper part of the gap.

We note that it is difficult to pinpoint the exact cause of the Fermi level shift, as given the need to do PES measurements on a conducting substrate, we are unable to measure the perovskite on glass. However, it is likely that both effects, in concert, result in Fermi level shift which we have observed. Thus, the overarching effective result here is that the work function change which we measure on the perovskite surface (as a result of treating the surface of the SnO_2 with $BMIMBF_4$) is due to a shift in the Fermi-level of the perovskite towards the conduction band, i.e., the perovskite has a more "n-type" character.

To show how this would affect charge carrier extraction, we perform PLQE measurements of half-cells (FTO/SnO_2/perovskite/PMMA) fabricated with neat, and IL-treated SnO_2 (**Figure S4**). This experiment, as with the neat perovskite films, shows an increase in the photoluminescence of the half-cells with the IL-modified substrates, indicating a reduction of non-radiative recombination in the presence of a perovskite/SnO_2 interface. Using absolute photoluminescence yield measurements, Stolterfoht et al. have shown that suppressing interfacial recombination losses is crucial for maximizing the quasi-Fermi level splitting and thus improving the open-circuit voltage.[60] The increase in PLQE in the half-cells is indicative of the IL treatment resulting in a reduction of those loss pathways. To probe the effect of this treatment on full perovskite solar cells, we fabricate planar n-i-p devices with the following architecture: FTO/SnO_2/$BMIMBF_4$/perovskite/spiro-OMeTAD/Au.

Pursuant to the DOE Public Access Plan, this document represents the authors' peer-reviewed, accepted manuscript.
The published version of the article is available from the relevant publisher.

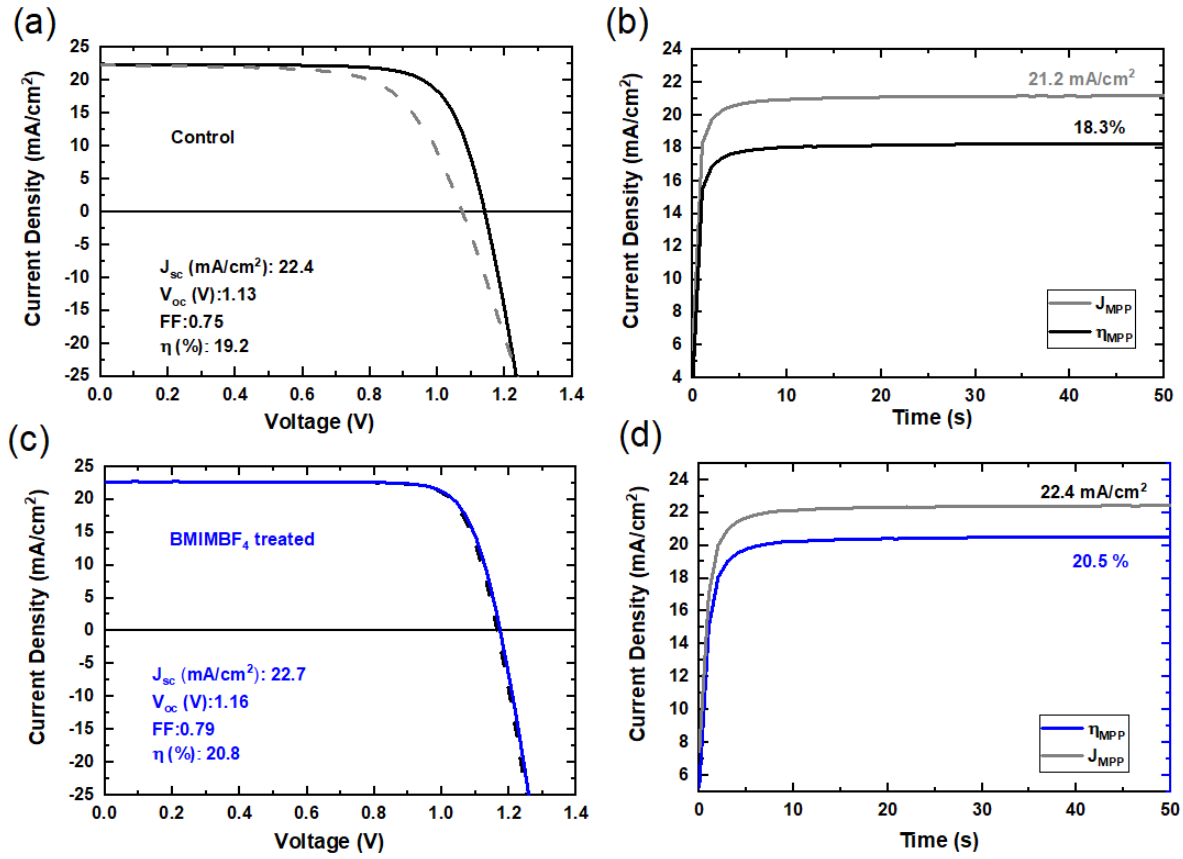

Figure 5. Current-Voltage Characteristics. Current-Voltage characteristics of $FA_{0.83}MA_{0.17}Pb(I_{0.83}Br_{0.17})_3$ solar cells fabricated on (a) neat and (c) $BMIMBF_4$-treated SnO_2 substrates. (b) and (d) Steady-state current and efficiency measurements of the devices shown in (a) and (c) respectively.

We start out by varying the concentration of $BMIMBF_4$ deposited on the SnO_2. We find that while treating the SnO_2 with low concentrations of $BMIMBF_4$ results in an improvement in the performance of the devices, at concentrations above 0.01 wt.% in a methanol solution, there is a decrease in device performance (See **Figure S5**). This decrease in performance is likely due to the deposition of too thick a layer of IL on the surface of the SnO_2, which presumably hinders charge extraction, or adversely affects the perovskite crystallisation at this interface. We show the *JV* characteristics of the best-performing control, and IL-treated devices in **Figure 5**, and the external quantum efficiency of these devices in **Figure S6**. While the short circuit current (J_{SC}) of these devices is comparable (22.4 mA/cm^2 vs. 22.7 mA/cm^2), there is a notable increase in the open-circuit voltage (V_{OC}) and the fill-factor (FF) of the treated samples, which is accompanied by a significant decrease in the hysteresis of the JV curves. This is also reflected in the increase of the steady-state efficiency of the devices, measured by holding the device at its maximum power point (MPP) voltage, where the device efficiency increases from 18.3% to

Pursuant to the DOE Public Access Plan, this document represents the authors' peer-reviewed, accepted manuscript.
The published version of the article is available from the relevant publisher.

20.5%. These improvements are fully consistent with the suppression of interfacial recombination losses which, to a large degree, contribute to voltage-losses and influence the severity of the *JV*-hysteresis.[60,61] The results are also in good agreement with those obtained by Chang et al, when treating the surface of TiO_2 with ILs. The explanation given for the device improvement in their work focused largely on the effect on the IL on the metal-oxide, but it largely ignored any potential interaction between the IL and the perovskite absorber. However, given the change in the WF of the perovskite which we have observed, we can now confidently expand the explanation for the observed performance improvements in these systems, to include the induction of a more n-type nature, and reduction in the density of active trap sites within the perovskite absorber.

Conclusion:

In conclusion, we have shown that the role of the ionic liquid, $BMIMBF_4$, in n-i-p perovskite solar cells is not only to passivate and modify the surface of the n-type oxide, but that the improvement observed also occurs as a result of a direct interaction between the ionic liquid and the halide perovskite. The inclusion of the ionic liquid layer results in a significant shift of the Fermi level towards higher binding energies which corresponds to a larger occupation of higher electronic states. In addition to the increase in the n-type nature of the perovskite, crystallising the perovskite on a $BMIMBF_4$ layer results in the filling, and hence the "passivation" or "neutralisation" of electronic trap states, which we demonstrate by measuring longer charge-carrier lifetimes and higher mobilities on the nanosecond to millisecond timescale. As a result, for solar cells where the perovskite absorber is crystallised upon the IL-modified contact layer, we observe reduced recombination losses in the form of an improvement in the V_{OC} and a reduction in the *JV* hysteresis. This study further highlights the importance of devising strategies to reduce the electron trap density in perovskite materials, one of which is the control and modification of the doping levels of the perovskite. Future studies are needed to identify the exact processes underlying these observed surface-dependent doping effects, thus allowing for more control and additional tailoring of the interfaces to further improve the performances of perovskite-based optoelectronic devices.

Supporting Information

Supporting Information is available from the Wiley Online Library or from the author.

Pursuant to the DOE Public Access Plan, this document represents the authors' peer-reviewed, accepted manuscript.
The published version of the article is available from the relevant publisher.

Acknowledgements

This work was partly funded by the Engineering and Physical Sciences Research Council, UK. NKN acknowledges funding *via* a fellowship from the Princeton Center for Complex Materials (PCCM). B. W. acknowledges funding from the European Commission *via* a Marie Skłodowska-Curie individual fellowship (REA Grant Number 706552-APPEL). A.K and F.Z gratefully acknowledge funding from the US Department of Energy. S. N. H. was supported by the Director's Fellowship program of the National Renewable Energy Laboratory under Contract No. DE-AC36-08GO28308.This work was authored in part by Alliance for Sustainable Energy, LLC, the manager and operator of the National Renewable Energy Laboratory for the U.S. Department of Energy (DOE) under Contract No. DE-AC36-08GO28308. The views expressed in the article do not necessarily represent the views of the DOE or the U.S. Government. The authors acknowledge the use of Princeton's Imaging and Analysis Center (IAC), which is partially supported by the Princeton Center for Complex Materials, a National Science Foundation (NSF) Materials Research Science and Engineering Center (MRSEC; DMR-1420541).

Received: ((will be filled in by the editorial staff))
Revised: ((will be filled in by the editorial staff))
Published online: ((will be filled in by the editorial staff))

References:

[1] A. Kojima, K. Teshima, Y. Shirai, T. Miyasaka, *J. Am. Chem. Soc.* **2009**, *131*, 6050.

[2] N. R. E. L. (NREL), "Best Research-Cell Efficiencies," can be found under https://www.nrel.gov/pv/assets/pdfs/best-research-cell-efficiencies-190416.pdf, **2019**.

[3] M. M. Lee, J. Teuscher, T. Miyasaka, T. N. Murakami, H. J. Snaith, *Science* **2012**, *338*, 643.

[4] S. D. Stranks, G. E. Eperon, G. Grancini, C. Menelaou, M. J. P. Alcocer, T. Leijtens, L. M. Herz, A. Petrozza, H. J. Snaith, *Science* **2013**, *342*, 341.

[5] S. D. Stranks, H. J. Snaith, *Nat. Nanotechnol.* **2015**, *10*, 391.

[6] N. K. Noel, S. D. Stranks, A. Abate, C. Wehrenfennig, S. Guarnera, A.-A. Haghighirad, A. Sadhanala, G. E. Eperon, S. K. Pathak, M. B. Johnston, A. Petrozza, L. M. Herz, H. J. Snaith, *Energy Environ. Sci.* **2014**, *7*, 3061.

Pursuant to the DOE Public Access Plan, this document represents the authors' peer-reviewed, accepted manuscript. The published version of the article is available from the relevant publisher.

[7] C. L. Davies, M. R. Filip, J. B. Patel, T. W. Crothers, C. Verdi, A. D. Wright, R. L. Milot, F. Giustino, M. B. Johnston, L. M. Herz, *Nat. Commun.* **2018**, *9*, 293.

[8] H.-S. Kim, C.-R. Lee, J.-H. Im, K.-B. Lee, T. Moehl, A. Marchioro, S.-J. Moon, R. Humphry-Baker, J.-H. Yum, J. E. Moser, M. Grätzel, N.-G. Park, *Sci. Rep.* **2012**, *2*, 591.

[9] J. M. Ball, M. M. Lee, A. Hey, H. Snaith, *Energy Environ. Sci.* **2013**.

[10] G. E. Eperon, V. M. Burlakov, P. Docampo, A. Goriely, H. J. Snaith, *Adv. Funct. Mater.* **2014**, *24*, 151.

[11] M. Liu, M. B. Johnston, H. J. Snaith, *Nature* **2013**, *501*, 395.

[12] M. Xiao, F. Huang, W. Huang, Y. Dkhissi, Y. Zhu, J. Etheridge, A. Gray-Weale, U. Bach, Y.-B. Cheng, L. Spiccia, *Angew. Chemie* **2014**, *126*, 10056.

[13] W. Nie, H. Tsai, R. Asadpour, J.-C. Blancon, A. J. Neukirch, G. Gupta, J. J. Crochet, M. Chhowalla, S. Tretiak, M. A. Alam, H.-L. Wang, A. D. Mohite, *Science* **2015**, *347*, 522.

[14] N. K. Noel, S. N. Habisreutinger, B. Wenger, M. T. Klug, M. T. Horantner, M. B. Johnston, R. J. Nicholas, D. T. Moore, H. J. Snaith, *Energy Environ. Sci.* **2017**, *10*, 145.

[15] D. P. McMeekin, Z. Wang, W. Rehman, F. Pulvirenti, J. B. Patel, N. K. Noel, M. B. Johnston, S. R. Marder, L. M. Herz, H. J. Snaith, *Adv. Mater.* **2017**, *29*, 1607039.

[16] N. K. Noel, B. Wenger, S. N. Habisreutinger, J. B. Patel, T. Crothers, Z. Wang, R. J. Nicholas, M. B. Johnston, L. M. Herz, H. J. Snaith, *ACS Energy Lett.* **2018**, *3*, 1233.

[17] P. Schulz, D. Cahen, A. Kahn, *Chem. Rev.* **2019**, *119*, 3349.

[18] I. Zarazua, G. Han, P. P. Boix, S. Mhaisalkar, F. Fabregat-Santiago, I. Mora-Seró, J. Bisquert, G. Garcia-Belmonte, *J. Phys. Chem. Lett.* **2016**, *7*, 5105.

[19] Y. Yang, M. Yang, D. T. Moore, Y. Yan, E. M. Miller, K. Zhu, M. C. Beard, *Nat. Energy* **2017**, *2*, 16207.

[20] M. Stolterfoht, C. M. Wolff, J. A. Márquez, S. Zhang, C. J. Hages, D. Rothhardt, S. Albrecht, P. L. Burn, P. Meredith, T. Unold, D. Neher, *Nat. Energy* **2018**, *3*, 847.

[21] N. K. Noel, A. Abate, S. D. Stranks, E. S. Parrott, V. M. Burlakov, A. Goriely, H. J. Snaith, *ACS Nano* **2014**, *8*, 9815.

[22] X. Zheng, B. Chen, J. Dai, Y. Fang, Y. Bai, Y. Lin, H. Wei, X. C. Zeng, J. Huang, *Nat. Energy* **2017**, *2*, 17102.

[23] J. A. Christians, P. Schulz, J. S. Tinkham, T. H. Schloemer, S. P. Harvey, B. J. Tremolet de Villers, A. Sellinger, J. J. Berry, J. M. Luther, *Nat. Energy* **2018**, *3*, 68.

Pursuant to the DOE Public Access Plan, this document represents the authors' peer-reviewed, accepted manuscript. The published version of the article is available from the relevant publisher.

[24] N. K. Noel, S. N. Habisreutinger, A. Pellaroque, F. Pulvirenti, B. Wenger, F. Zhang, Y.-H. Lin, O. G. Reid, J. Leisen, Y. Zhang, S. Barlow, S. R. Marder, A. Kahn, H. J. Snaith, C. B. Arnold, B. P. Rand, *Energy Environ. Sci.* **2019**, *12*, 3063.

[25] S. N. Habisreutinger, N. K. Noel, B. W. Larson, O. G. Reid, J. L. Blackburn, *ACS Energy Lett.* **2019**, *4*, 1872.

[26] I. L. Braly, D. W. deQuilettes, L. M. Pazos-Outón, S. Burke, M. E. Ziffer, D. S. Ginger, H. W. Hillhouse, *Nat. Photonics* **2018**, *12*, 355.

[27] D. W. de Quilettes, S. M. Vorpahl, S. D. Stranks, H. Nagaoka, G. E. Eperon, M. E. Ziffer, H. J. Snaith, D. S. Ginger, *Science* **2015**, *348*, 683.

[28] K. Wojciechowski, T. Leijtens, S. Siprova, C. Schlueter, M. T. Hörantner, J. T.-W. Wang, C.-Z. Li, A. K. Y. Jen, T.-L. Lee, H. J. Snaith, *J. Phys. Chem. Lett.* **2015**, *6*, 2399.

[29] Z. Wang, D. P. McMeekin, N. Sakai, S. van Reenen, K. Wojciechowski, J. B. Patel, M. B. Johnston, H. J. Snaith, *Adv. Mater.* **2017**, *29*, 1604186.

[30] A. Pellaroque, N. K. Noel, S. N. Habisreutinger, Y. Zhang, S. Barlow, S. R. Marder, H. J. Snaith, *ACS Energy Lett.* **2017**, *2*, 2044.

[31] F. Pulvirenti, B. Wegner, N. K. Noel, G. Mazzotta, R. Hill, J. B. Patel, L. M. Herz, M. B. Johnston, M. K. Riede, H. J. Snaith, N. Koch, S. Barlow, S. R. Marder, *Mol. Syst. Des. Eng.* **2018**, DOI 10.1039/C8ME00031J.

[32] Z. Wang, D. P. McMeekin, N. Sakai, S. van Reenen, K. Wojciechowski, J. B. Patel, M. B. Johnston, H. J. Snaith, *Adv. Mater.* **2017**, *29*, 1604186.

[33] N. K. Noel, M. Congiu, A. J. Ramadan, S. Fearn, D. P. McMeekin, J. B. Patel, M. B. Johnston, B. Wenger, H. J. Snaith, *Joule* **2018**, *1*, 328.

[34] W. Zhang, S. Pathak, N. Sakai, T. Stergiopoulos, P. K. Nayak, N. K. Noel, A. A. Haghighirad, V. M. Burlakov, D. W. deQuilettes, A. Sadhanala, W. Li, L. Wang, D. S. Ginger, R. H. Friend, H. J. Snaith, *Nat Commun* **2015**, *6*, DOI 10.1038/ncomms10030.

[35] J. T.-W. Wang, Z. Wang, S. Pathak, W. Zhang, D. W. deQuilettes, F. Wisnivesky-Rocca-Rivarola, J. Huang, P. K. Nayak, J. B. Patel, H. A. Mohd Yusof, Y. Vaynzof, R. Zhu, I. Ramirez, J. Zhang, C. Ducati, C. Grovenor, M. B. Johnston, D. S. Ginger, R. J. Nicholas, H. J. Snaith, *Energy Environ. Sci.* **2016**, *9*, 2892.

[36] K. Yan, M. Long, T. Zhang, Z. Wei, H. Chen, S. Yang, J. Xu, *J. Am. Chem. Soc.* **2015**, *137*, 4460.

[37] E. H. Anaraki, A. Kermanpur, L. Steier, K. Domanski, T. Matsui, W. Tress, M. Saliba, A. Abate, M. Gratzel, A. Hagfeldt, J.-P. Correa-Baena, *Energy Environ. Sci.* **2016**, *9*,

Pursuant to the DOE Public Access Plan, this document represents the authors' peer-reviewed, accepted manuscript. The published version of the article is available from the relevant publisher.

3128.

[38] J. P. Correa Baena, L. Steier, W. Tress, M. Saliba, S. Neutzner, T. Matsui, F. Giordano, T. J. Jacobsson, A. R. Srimath Kandada, S. M. Zakeeruddin, A. Petrozza, A. Abate, M. K. Nazeeruddin, M. Gratzel, A. Hagfeldt, *Energy Environ. Sci.* **2015**, *8*, 2928.

[39] J.-Y. Seo, T. Matsui, J. Luo, J.-P. Correa-Baena, F. Giordano, M. Saliba, K. Schenk, A. Ummadisingu, K. Domanski, M. Hadadian, A. Hagfeldt, S. M. Zakeeruddin, U. Steiner, M. Grätzel, A. Abate, *Adv. Energy Mater.* **2016**, *6*, 1600767.

[40] Y. Wu, F. Xie, H. Chen, X. Yang, H. Su, M. Cai, Z. Zhou, T. Noda, L. Han, *Adv. Mater.* **2017**, *29*, 1701073.

[41] D. Yang, X. Zhou, R. Yang, Z. Yang, W. Yu, X. Wang, C. Li, S. (Frank) Liu, R. P. H. Chang, *Energy Environ. Sci.* **2016**, *9*, 3071.

[42] Q. Wu, W. Zhou, Q. Liu, P. Zhou, T. Chen, Y. Lu, Q. Qiao, S. Yang, *ACS Appl. Mater. Interfaces* **2016**, *8*, 34464.

[43] D. Yang, R. Yang, X. Ren, X. Zhu, Z. Yang, C. Li, S. (Frank) Liu, *Adv. Mater.* **2016**, *28*, 5206.

[44] M. Li, C. Zhao, Z.-K. Wang, C.-C. Zhang, H. K. H. Lee, A. Pockett, J. Barbé, W. C. Tsoi, Y.-G. Yang, M. J. Carnie, X.-Y. Gao, W.-X. Yang, J. R. Durrant, L.-S. Liao, S. M. Jain, *Adv. Energy Mater.* **2018**, *8*, 1801509.

[45] S. Bai, P. Da, C. Li, Z. Wang, Z. Yuan, F. Fu, M. Kawecki, X. Liu, N. Sakai, J. T.-W. Wang, S. Huettner, S. Buecheler, M. Fahlman, F. Gao, H. J. Snaith, *Nature* **2019**, *571*, 245.

[46] J. Chen, X. Zhao, S.-G. Kim, N.-G. Park, *Adv. Mater.* **2019**, *0*, 1902902.

[47] P. Schulz, L. L. Whittaker-Brooks, B. A. MacLeod, D. C. Olson, Y.-L. Loo, A. Kahn, *Adv. Mater. Interfaces* **2015**, *2*, 1400532.

[48] E. M. Miller, Y. Zhao, C. C. Mercado, S. K. Saha, J. M. Luther, K. Zhu, V. Stevanović, C. L. Perkins, J. van de Lagemaat, *Phys. Chem. Chem. Phys.* **2014**, *16*, 22122.

[49] S. Braun, W. R. Salaneck, M. Fahlman, *Adv. Mater.* **2009**, *21*, 1450.

[50] J. Endres, M. Kulbak, L. Zhao, B. P. Rand, D. Cahen, G. Hodes, A. Kahn, *J. Appl. Phys.* **2017**, *121*, 35304.

[51] M. Saba, M. Cadelano, D. Marongiu, F. Chen, V. Sarritzu, N. Sestu, C. Figus, M. Aresti, R. Piras, A. Geddo Lehmann, C. Cannas, A. Musinu, F. Quochi, A. Mura, G. Bongiovanni, *Nat. Commun.* **2014**, *5*, 5049.

[52] J. M. Ball, A. Petrozza, *Nat. Energy* **2016**, *1*, 16149.

[53] T. Leijtens, G. E. Eperon, A. J. Barker, G. Grancini, W. Zhang, J. M. Ball, A. R. S.

Pursuant to the DOE Public Access Plan, this document represents the authors' peer-reviewed, accepted manuscript. The published version of the article is available from the relevant publisher.

Kandada, H. J. Snaith, A. Petrozza, *Energy Environ. Sci.* **2016**, *9*, 3472.

[54] B. Wenger, P. K. Nayak, X. Wen, S. V Kesava, N. K. Noel, H. J. Snaith, *Nat. Commun.* **2017**, *8*, 590.

[55] D. Ramirez, K. Schutt, J. F. Montoya, S. Mesa, J. Lim, H. J. Snaith, F. Jaramillo, *J. Phys. Chem. C* **2018**, *122*, 21239.

[56] A. Dai, Y. Zhou, A. L. Shu, S. K. Mohapatra, H. Wang, C. Fuentes-Hernandez, Y. Zhang, S. Barlow, Y.-L. Loo, S. R. Marder, B. Kippelen, A. Kahn, *Adv. Funct. Mater.* **2013**, *24*, 2197.

[57] S. Olthof, K. Meerholz, *Sci. Rep.* **2017**, *7*, 40267.

[58] A. Zohar, M. Kulbak, I. Levine, G. Hodes, A. Kahn, D. Cahen, *ACS Energy Lett.* **2019**, *4*, 1.

[59] S. D. Stranks, V. M. Burlakov, T. Leijtens, J. M. Ball, A. Goriely, H. J. Snaith, *Phys. Rev. Appl.* **2014**, *2*, 34007.

[60] M. Stolterfoht, P. Caprioglio, C. M. Wolff, J. A. Márquez, J. Nordmann, S. Zhang, D. Rothhardt, U. Hörmann, A. Redinger, L. Kegelmann, S. Albrecht, T. Kirchartz, M. Saliba, T. Unold, D. Neher, *arXiv Prepr. arXiv1810.01333* **2018**, *35*, 423.

[61] S. N. Habisreutinger, N. K. Noel, H. J. Snaith, *ACS Energy Lett.* **2018**, *3*, 2472.

Pursuant to the DOE Public Access Plan, this document represents the authors' peer-reviewed, accepted manuscript. The published version of the article is available from the relevant publisher.

Copyright WILEY-VCH Verlag GmbH & Co. KGaA, 69469 Weinheim, Germany, 2018.

Crystallising perovskites on an ionic liquid-modified SnO_2 substrate causes a shift of the perovskite Fermi level toward the conduction band and decreases the density of trap states in the perovskite. This results in a reduction of non-radiative recombination losses and, consequently, improved solar cell efficiencies.

TOC Keywords: solar cells, surface modification

Elucidating the Role of a Tetrafluoroborate-based Ionic Liquid at the n-Type Oxide/Perovskite Interface

Nakita K. Noel,[1,2*] Severin N. Habisreutinger,[3] Bernard Wenger,[4] Yen-Hung Lin,[4] Fengyu Zhang,[2] Jay B. Patel,[4] Antoine Kahn,[2] Michael B. Johnston,[4] Henry J. Snaith.[4*]

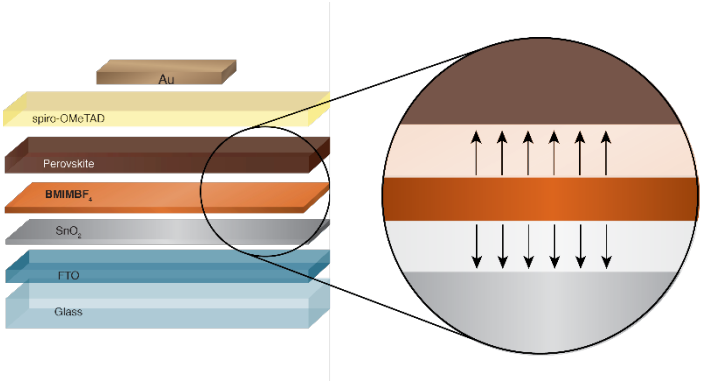

Pursuant to the DOE Public Access Plan, this document represents the authors' peer-reviewed, accepted manuscript.
The published version of the article is available from the relevant publisher.